

Draft Dated: Monday, August 25, 2003

Contents of Chapter 23

1. Introduction
2. Fluid-Structure Interaction
3. Finite Element Model Of Dam-Foundation Interface
4. Loading Due To Uplift And Pore Water Pressure
5. Pore Water Pressure Calculation Using Sap2000
6. Selection Of Gap Element Stiffness Value
7. Fundamental Equations In Fluid Dynamics
8. Relationship Between Pressure And Velocity
9. Equilibrium At The Interface Of Two Materials
10. Radiation Boundary Conditions
11. Surface Sloshing Modes
12. Vertical Wave Propagation
13. The Westergaard Paper
14. Dynamic Analysis of Rectangular Reservoir
15. Finite Element Modeling of Energy Absorptive Reservoir Boundaries
16. Relative Versus Absolute Form
17. The Effect Of Gate Setback On Pressure
18. Seismic Analysis of Radial Gates
19. Final Remarks

23.

FLUID-STRUCTURE INTERACTION

A Confined Fluid can be considered as a Special Case of a Solid Material. Since, Fluid has a Very Small Shear Modulus Compared to it's Compressibility Modulus

23.1 INTRODUCTION

The static and dynamic finite element analysis of systems, such as dams, that contain both fluid and solid elements can be very complex. Creating a finite element model of fluid-solid systems that accurately simulates the behavior of the real physical system, requires the engineer/analysts to make many approximations. Therefore, the purpose of this chapter is to present a logical approach to the selection of the finite element model and to suggest parameter studies in order to minimize the errors associated with various approximations. Figure 23.1 illustrates a typical fluid/solid/foundation dam structural system and illustrates the several approximations that are required in order to create a realistic finite element model for both static and dynamic loads.

23-2 STATIC AND DYNAMIC ANALYSIS

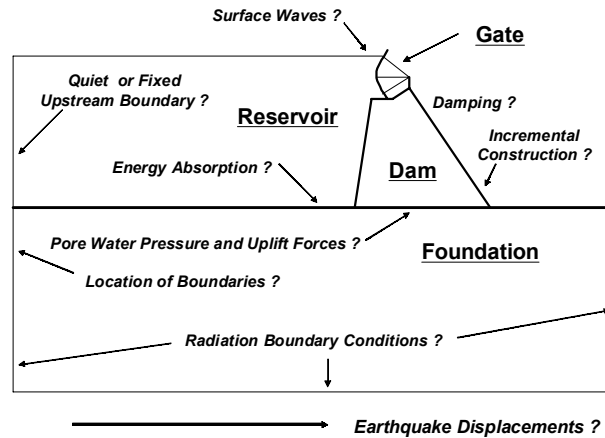


Figure 23.1. Approximations required for the Creation of a Finite Element Model For Fluid/Solid Systems

This example involves, in many cases, the use of orthotropic, layered foundation. The dam is constructed incrementally, often over a several month period, where the material properties, temperature and creep are a function of time. Therefore, the determination of the dead-load stress distribution within the dam can be relatively complicated. For gravity dams the dead load stresses from an incremental analysis may not be significantly different from the results of an analysis due to the dead load applied to the complete dam instantaneously. However, for narrow arch dams the instantaneous application of the dead load to the complete dam can cause erroneous vertical tension stresses near the abutments at the top of the dam.

SAP2000 has an incremental construction option that can be activated by the user in order to accurately model the construction sequence. In addition, SAP2000 has the ability to model most of the boundary conditions shown in Figure 23.1. Also, frame elements, solid elements and fluid elements can be used in the same model; hence, it is possible to capture the complex interaction between foundation, dam, reservoir and attached structures such as gates, bridges and intake towers.

23.2 FLUID-STRUCTURE INTERACTION

It has been standard practice to assume that fluid is incompressible for many fluid-structure interaction problems. As a result of the assumptions of incompressible fluid and a rigid structure, many dynamic fluid-structure interaction problems have been approximately solved replacing the fluid with an *added mass*. Also, the incompressible approximation allowed many problems, of simple geometry, to be solved in closed form using classical mathematical methods. However, the incompressible approximation can cause significant errors for high frequency loading and is no longer required due to the development of alternate fluid finite elements that can be used to accurately model complex geometric shapes. In Chapter 6, a three-dimensional 8-node solid element, with incompatible displacement modes, allows confined fluid systems to be accurately modeled by using the exact compressibility of water and a very low shear modulus. Table 23.1 summarizes the properties of water and two other materials with small shear moduli. In a displacement based finite element analysis it is not possible to use a zero shear modulus. However, a small value can be used without the introduction of significant errors.

Table 23.1. Approximate Mechanical Properties of Water

G/λ Ratio	E Young's Modulus ksi	ν Poisson's Ratio	G Shear Modulus ksi	λ Bulk Modulus ksi	w Weight Density lb/ft ³
0.000	0	0.50000	0.00	300	62.4
0.0001	0.090	0.49995	0.03	300	62.4
0.0010	0.900	0.49950	0.30	300	62.4
0.0100	9.000	0.49500	3.00	300	62.4

In order to illustrate the ability of the solid element to model fluid behavior consider the reservoir system, subjected to the static dead load only, as shown in Figure 23.2.

23-4 STATIC AND DYNAMIC ANALYSIS

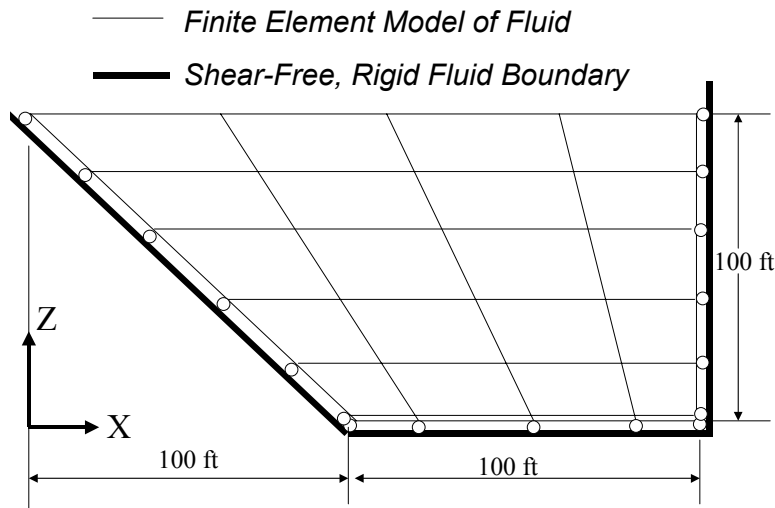


Figure 23.2. Hydrostatic Load Analysis of Reservoir Model

Note that a very thin element has been placed at the base of the reservoir in order that accurate fluid pressures can be calculated. For this simple example the exact hydrostatic pressure near the base of the dam is 43.33 psi and the total hydrostatic horizontal force acting on the right vertical boundary is 312 kips per foot of thickness. The total horizontal reactive force and the approximate stresses obtained from the finite element model, using three different material properties, are summarized in Table 23.2.

Table 23.2. Hydrostatic Load Analysis using Fluid Finite Elements

G Shear Modulus ksi	λ Bulk Modulus ksi	Force Acting on Right Boundary kips	Stresses in Fluid at Base of Dam - psi			
			σ_{xx}	σ_{yy}	σ_{zz}	τ_{xz}
0.0 (exact)	300	312.0	43.33	43.33	43.33	0.00
0.03	300	310.2	43.47	43.68	43.48	0.0002
0.3	300	309.6	43.41	43.40	43.48	.002
3.0	300	307.3	42.82	42.72	43.49	.025

The approximate stresses obtained using fluid elements with small shear moduli are very close to the exact hydrostatic pressure. The total horizontal force acting on the right boundary is more sensitive to the use of a small finite shear modulus. However, the error is less than one percent if the shear modulus is less or equal to 0.1 percent of the bulk modulus. Therefore, this is the value of shear modulus that is recommended for reservoir/dam interaction analysis.

In the case of a dynamic analysis of a system of fluid finite elements, the addition to the exact mass of the fluid does not introduce any additional approximations. Since the viscosity of the fluid is normally ignored in a dynamic analysis the use of a small shear modulus may produce more realistic results. Prior to any dynamic, hydrostatic loading must be applied in order to verify the accuracy and boundary conditions of the fluid-structure finite element model.

23.3 FINITE ELEMENT MODEL OF DAM-FOUNDATION INTERFACE

At the intersection of the upstream (or downstream) face of the dam with the foundation, a stress concentration exists. A very fine mesh solution, for any load condition, would probably indicate very large stresses. A further refinement of the mesh would just produce higher stresses. However, due to the nonlinear behavior of both the concrete and foundation material these high stresses cannot exist in the real structure. Hence, it is necessary to select a finite element model that predicts the overall behavior of the structure without indicating a high stress concentration that cannot exist in the real structure.

One of the difficulties in creating a realistic finite element model is that we do not fully understand the physics of the real behavior of the dam-foundation-reservoir when the system is subjected to earthquake displacements. For example, if tension causes uplift at the dam-foundation interface, can shear still be transferred? Also, do the uplift water pressures change during loading? Because of these and other unknown factors we must use good engineering judgment and conduct several different finite element models using different assumptions.

The author has had over 40 years experience in the static and dynamic finite element analysis of dams and many other types of structures. Based on this

23-6 STATIC AND DYNAMIC ANALYSIS

experience, Figure 3 shows a typical finite element model at the interface between the dam and foundation.

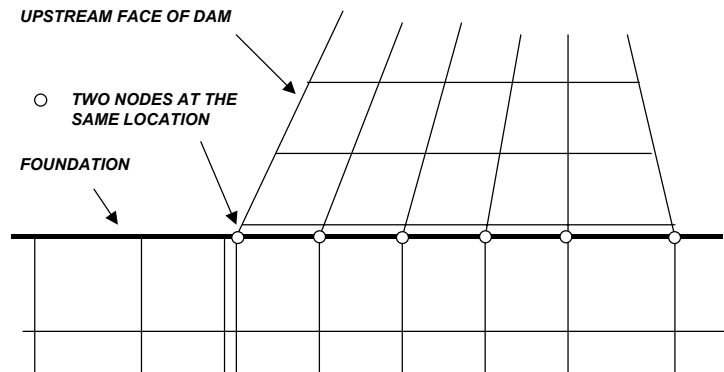


Figure 23.3. Finite Element Model of a Dam-Foundation Interface

A simple method to create a finite element model of a dam and foundation is to use eight-node solid elements for both the dam and foundation. In order to obtain the best accuracy it is preferable to use regular quadrilateral types of meshes whenever possible.

Note that it is always necessary to use two nodes at all interfaces between two different material properties. This is because the stresses parallel to the interface of different materials are not equal. Therefore, two nodes at the interface are required in order for SAP2000 to plot accurate stress contours. The nodes must be located at the same point in space. However, after the two meshes for the dam and foundation are created the two nodes at the interface can be constrained to have equal displacements.

Another advantage of placing two nodes at the interface is that it may be necessary to place nonlinear *gap elements* at these locations in order to allow uplift in a subsequent nonlinear dynamic analysis. However, it is strongly recommended that a *static-load, linear analysis* always be conducted prior to any nonlinear analysis. This will allow the engineer to check the validity of the finite element model prior to a linear or nonlinear dynamic analysis.

The finite element model shown in Figure 3 indicates a layer of thin solid elements (approximately 10 cm thick) at the base of the dam since this is where the maximum stresses will exist. Also, in order to allow consistent foundation displacements it is recommended that a vertical layer of smaller elements be placed in the foundation as shown.

Normal hydrostatic loading is often directly applied to the top of the foundation and the upstream face of the dam. If this type of surface loading is applied, large horizontal tension stresses will exist in the foundations and vertical tension stresses will exist at the upstream surface of the dam. In other words, the surface hydrostatic loading tends to tear the dam from the foundation.

In the next section a more realistic approach will be suggested for the application of hydrostatic loads that should reduce these unrealistic stresses and produce a more accurate solution. The correct approach is to use a pore water pressure approach that is physically realistic.

23.4 LOADING DUE TO UPLIFT AND PORE WATER PRESSURE

In the static analysis of gravity dam structures it is possible to approximate the uplift forces by a simple uplift pressure acting at the base of the dam. However, if the dam and foundation are modeled by finite elements this simple approximation cannot be used. The theoretically correct approach is to first evaluate the pore water pressure at all points within the dam and foundation as shown in Figure 23.4a. The SAP2000 program has an option to perform such calculations.

23-8 STATIC AND DYNAMIC ANALYSIS

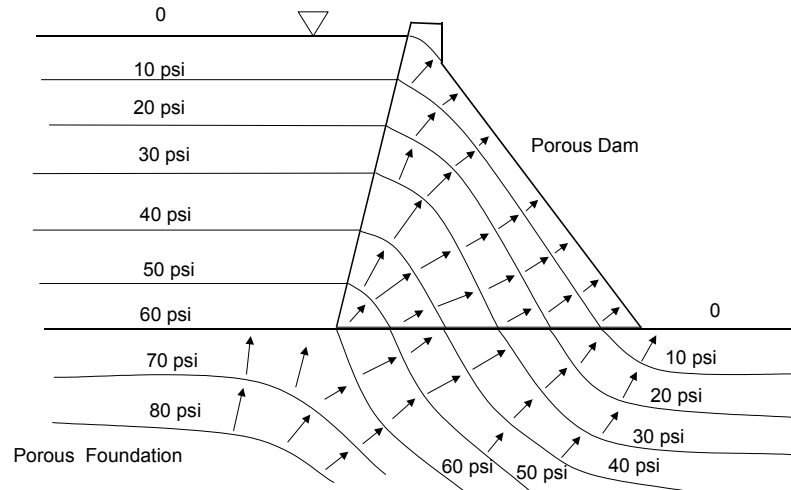


Figure 23.4a. Water Pressure within Dam, Reservoir and Foundation

The loads associated with the pore water pressure $p(x, y, z)$ only exist if there are pressure gradients $\frac{dp}{dx}$, $\frac{dp}{dy}$ or $\frac{dp}{dz}$. Therefore, in three-dimensions the differential forces are transferred from the water to the solid material and are given by

$$\begin{aligned}
 df_x &= -\frac{dp}{dx} dV \\
 df_y &= -\frac{dp}{dy} dV \\
 df_z &= -\frac{dp}{dz} dV
 \end{aligned}
 \tag{23.1}$$

Where df_i is the body force in the "i" direction acting on the volume dV . The pore water pressure loads can be treated as body forces within the standard finite element formulation and are consistently converted to node point loads as illustrated in Chapter. The approximate direction of these forces within the dam and foundation are shown in Figure 23.4b. The SAP2000 program has the ability

to calculate pore water loading automatically and these forces can be calculated for both static and dynamic analysis.

In order to illustrate that the simple strength of materials approach produces the same loading as the formal finite element method, consider the model shown in Figure 4b. For this case the dam has zero porosity and the foundation material is very porous. If these pore water loads are applied to the finite element model of the dam the first layer of elements at the base of the dam will receive the appropriate hydrostatic and uplift loads due to the large gradient in pressures within these elements

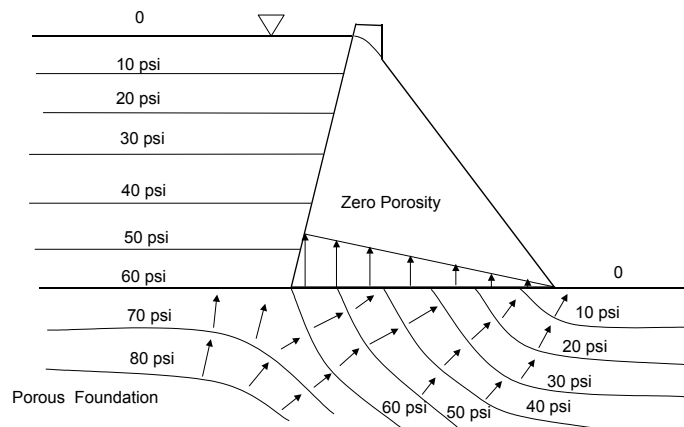


Figure 23.4b. Example of Uplift Forces Applied to Impervious Dam

If the foundation is also impervious, theoretically no uplift forces exist. However, experience indicates that water seepage takes place at the base along the dam-foundation interface that will cause uplift forces to act on the dam and downward forces to act on the foundation. The correct approach to the solution of this problem is to use nonlinear gap elements as shown in Figure 23.5.

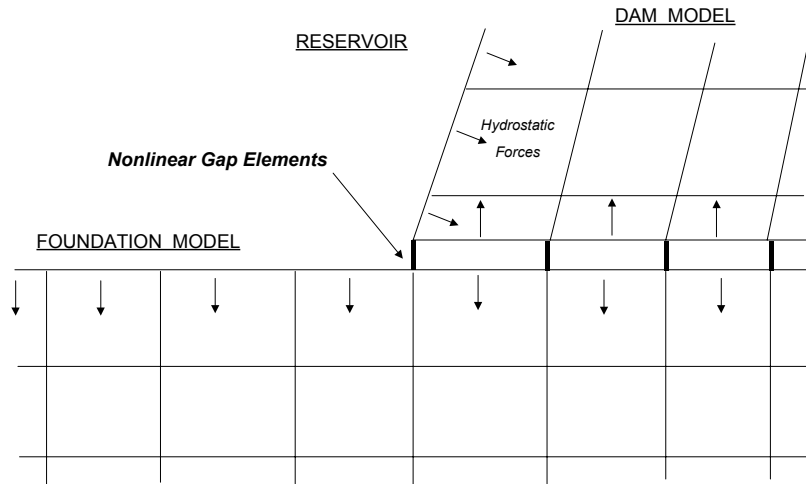


Figure 23.5. Uplift Model for Dam-Foundation System

Nonlinear gap elements cannot take tension forces. Under dead loads the elements will be in compression. However, after the application of the hydrostatic loads some of the gap elements may have zero forces (the SAP2000 program will automatically iterate at each time step to determine the correct force in the elements). The shear capacity of the element can be large or specified as a function of the normal force.

The theory and method of analysis presented in this section is based on the fundamental principles of physics and can be applied to both the static and dynamic analysis of dams.

23.5 PORE WATER PRESSURES CALCULATION USING SAP2000

For the case of steady state heat transfer or flow in porous media it is possible to use the SOLID element, without modification, to solve for the potential function and flows in the system. Because the element has orthotropic material it is possible to modify the material properties and to use the following analogy, summarized in Table 23.3, to solve this class of problems:

Table 23.3. Structural Analogy for the Solution of Potential Problems Using SAP2000**I STRUCTURAL ANALYSIS ANALOGY**

Let $u_x = u_y = 0$ and $u_z = P$, where P is the potential function.

The potential gradients are

$$P,x = u_{z,x} \quad \text{Analogous to the shear strain in the x-z plane.}$$

$$P,y = u_{z,y} \quad \text{Analogous to the shear strain in the y-z plane.}$$

$$P,z = u_{z,z} \quad \text{Analogous to the normal strain in the z-direction.}$$

The potential flow equations in terms of flow properties are

$$Q_x = k_x P,x \quad Q_y = k_y P,y \quad \text{and} \quad Q_z = k_z P,z$$

II COMPUTER PROGRAM INPUT

Therefore, the following material properties must be used in order to solve steady state flow problems in three-dimensions:

$$G_{xz} = k_x \quad G_{yz} = k_y \quad \text{and} \quad E_z = k_z$$

All other material properties are zero. The potential at a node is specified as a displacement u_z . A Concentrated node point flow into the system is specified as a positive node force in the z direction. Boundary points, that have zero external flows, have one unknown u_z .

III COMPUTER PROGRAM OUTPUT

u_z Equals the potential at the nodes.

τ_{xz} Equals the flow in the x direction within the element.

τ_{yz} Equals the flow in the y direction within the element.

σ_z Equals the flow in the z direction within the element.

The z-reactions are node point flows at points of specified potential.

23.6 SELECTION OF GAP ELEMENT STIFFNESS VALUE

The purpose of the nonlinear gap-element is to force surfaces within the computational model to transfer compression forces only and not allow tension forces to develop when the surfaces are not in contact. This can be accomplished by connecting nodes on two surfaces, located at the same point in space, with a gap element normal to the surface. The axial stiffness of the gap element must be selected large enough to transfer compression forces across the gap with a minimum of deformation within the gap element compared to the stiffness of the nodes on the surface. If the gap stiffness is too large, however, numerical problems can develop in the solution phase.

Modern personal computers conduct all calculations using 15 significant figures. If a gap element is 1000 times stiffer than the adjacent node stiffness then approximately 12 significant figures are retained to obtain an accurate solution. Therefore, it is necessary to estimate the normal stiffness at the interface surface nodes. The approximate surface node stiffness can be calculated from the following simple equation:

$$k = \frac{A_s E}{t_n} \quad (23.2)$$

Where A_s is the approximate surface area associated with the normal gap element, E is the modulus of elasticity of the dam and t_n is the finite element dimension normal to the surface. Hence, the gap-element stiffness is given by

$$k_g = 1000 \frac{A_s E}{t_n} \quad (23.3)$$

Increasing or decreasing this value by a factor of 10 should not change the results significantly.

23.7 FUNDAMENTAL EQUATIONS IN FLUID DYNAMICS

From Newton's Second Law the dynamic equilibrium equations, in terms of displacements u and fluid pressure p , for an infinitesimal fluid element are

$$p_{,x} = \rho \ddot{u}_x, \quad p_{,y} = \rho \ddot{u}_y \quad \text{and} \quad p_{,z} = \rho \ddot{u}_z \quad (23.4)$$

Where ρ is the mass density. The volume change ε of the infinitesimal fluid element in terms of the displacements is given by the following strain-displacement equation:

$$\varepsilon = \varepsilon_x + \varepsilon_y + \varepsilon_z = u_{x,x} + u_{y,y} + u_{z,z} \quad (23.5)$$

By definition the pressure-volume relationship for a fluid is

$$p = \lambda \varepsilon \quad (23.6)$$

Where λ is the bulk or compressibility modulus. Elimination of the pressure from Equations (23.4 and 23.6) produces the following three partial differential equations:

$$\begin{aligned} \rho \ddot{u}_x - \lambda(u_{x,xx} + u_{y,yx} + u_{z,zx}) &= 0 \\ \rho \ddot{u}_y - \lambda(u_{x,xy} + u_{y,yy} + u_{z,zy}) &= 0 \\ \rho \ddot{u}_z - \lambda(u_{x,xz} + u_{y,yz} + u_{z,zz}) &= 0 \end{aligned} \quad (23.7)$$

Consider the one-dimensional case $\rho \ddot{u}_x - \lambda u_{x,xx} = 0$. For one-dimensional, steady-state, wave propagation due to a harmonic pressure the solution is

$$\begin{aligned} u_x(x, t) &= u_o \text{Sin}(\omega t - \frac{\omega}{V} x) \quad t = -\infty \text{ to } +\infty \\ \ddot{u}_x(x, t) &= -u_o \omega^2 \text{Sin}(\omega t - \frac{\omega}{V} x) \\ u_{x,xx}(x, t) &= -u_o \frac{\omega^2}{V^2} \text{Sin}(\omega t - \frac{\omega}{V} x) \\ p &= u_{x,xx}(x, t) \lambda \end{aligned} \quad (23.8)$$

Substitution of the solution into the differential equation indicates the constant $V = \sqrt{\lambda/\rho}$ and is the speed at which a pressure wave propagates within the fluid. Therefore, the speed of wave propagation is $V = 4,719 \text{ ft/sec.}$ for water. Also, the wavelength wave is given by $L = V/f$ where f is the number of cycles per second of the pressure loading. For several different frequencies, the maximum values of displacements and pressures are summarized in Table 23.4 for a unit value of acceleration.

Table 23.4. One-Dimensional Wave Propagation in Water $\ddot{u}_0 = 1.0$

Loading Frequency f Cycles/Sec.	Loading Frequency $\omega = 2\pi f$ Rad./Sec.	Wave Length $L = V/f$ inches	Maximum Displacement $u_0 = 386.4/\omega^2$ inches	Maximum Pressure $p = \frac{\lambda \ddot{u}_g}{\omega V}$ psi
2	12.57	28,260	2.4455	163.2
5	31.42	11,304	0.3914	62.3
10	62.83	5,652	0.0938	32.6
20	125.7	2,826	0.0245	16.3
30	188.5	1,884	0.0108	10.9

Note that both the maximum displacements and the pressures are reduced as the frequency is increased for a compressible fluid.

23.8 RELATIONSHIP BETWEEN PRESSURE AND VELOCITY

One of the fundamental equations of fluid dynamics is the relationship between the fluid pressure and the velocity of the fluid at any point in space. In order to physically illustrate this relationship consider the fluid element shown in Figure 6. During a small increment of time Δt the one-dimensional wave will travel a distance $V\Delta t$ and the corresponding deformation of the element will be $\dot{u}\Delta t$. Therefore, the pressure can be expressed in terms of the velocity.

One-Dimensional Wave Propagation

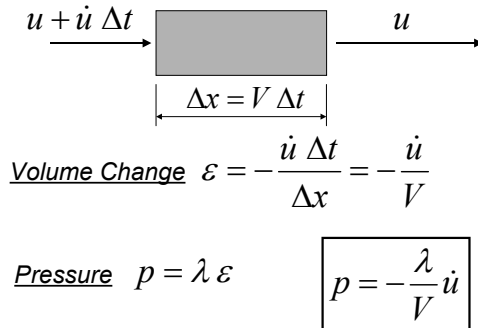


Figure 23.6. One-Dimensional Relationship Between Pressure and Velocity

The extension to three-dimensions yields

$$p(x, y, z) = -V\rho(\dot{u}_x + \dot{u}_y + \dot{u}_z) \tag{23.9}$$

Note that the direction of a propagating wave in a fluid is defined by a velocity vector with components \dot{u}_x , \dot{u}_y and \dot{u}_z .

23.9 EQUILIBRIUM AT THE INTERFACE OF TWO MATERIALS

Figure (23.7) summarizes the fundamental properties that are associated with the interface between two different materials. The bulk modulus and mass density of the material are λ and ρ respectively.

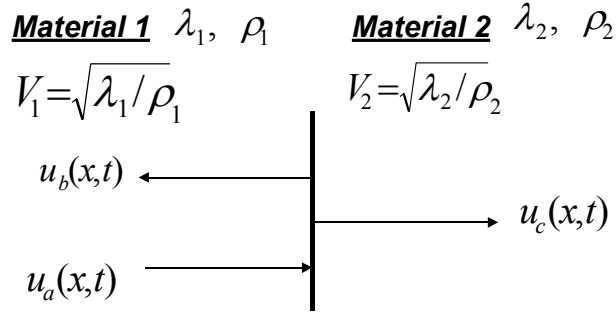


Figure 23.7. Wave propagation at a Material Interface

Velocity compatibility of particles on both sides of the interface requires that

$$\frac{du_a}{dt} + \frac{du_b}{dt} = \frac{du_c}{dt} \quad (10)$$

Rewriting Equation (23.9) we find that the three velocities can be expressed in terms of the pressures. Or,

$$\frac{du_a}{dt} = -\frac{V_1}{\lambda_1} p_a, \quad \frac{du_b}{dt} = \frac{V_1}{\lambda_1} p_b \quad \text{and} \quad \frac{du_c}{dt} = -\frac{V_2}{\lambda_2} p_c \quad (23.11)$$

Equilibrium of the pressure at the interface requires that

$$p_b = \alpha p_a \quad \text{and} \quad p_c = (1 + \alpha)p_a \quad (23.12)$$

Where α indicates the fraction of pressure of the incident wave that is reflected back from the interface.

Equation (10) can now be written as

$$(1 - \alpha) \frac{V_1}{\lambda_1} = (1 + \alpha) \frac{V_2}{\lambda_2} \quad (23.13)$$

Hence, α can be written in terms of the properties of the two materials as

$$\alpha = \frac{R-1}{R+1} \quad \text{where the material property ratio is } R = \sqrt{\frac{\lambda_2 \rho_2}{\lambda_1 \rho_1}} \quad (23.14)$$

Therefore, the value of α varies between 1 and -1 . If $\alpha = 1$, the boundary is rigid and does not absorb energy and the wave is reflected 100 percent back into the reservoir. If the materials are the same $\alpha = 0$ and the energy is completely dissipated and there is no reflection. If $\alpha = -1$, the boundary is very soft, compared to the bulk modulus of water, and does not absorb energy and the wave is reflected 100 percent back into the reservoir with a phase reversal.

If the value of α is known, then the material properties of material 2 can be written in terms of the material properties of material 1 and the known value of α . Or,

$$\sqrt{\lambda_2 \rho_2} = \frac{1+\alpha}{1-\alpha} \sqrt{\lambda_1 \rho_1} \quad (23.15)$$

23.10 RADIATION BOUNDARY CONDITIONS

From Figure 23.6. the pressure, as a function of time and space, can be written for one-dimensional wave propagation as

$$p(x,t) = \lambda \varepsilon = -V \rho \dot{u}_x(x,t) \quad (23.16)$$

Hence, the pressure is related to the absolute velocity by a viscous damping constant equal to the $V\rho$ per unit area. Therefore, linear viscous dash pots can be inserted at the upstream nodes of the reservoir that will allow the wave to pass and the strain energy in the water to “radiate” away from the dam. However, near the surface of the reservoir this is only approximate since a vertical velocity can exist which will alter the horizontal pressure.

23.11 SURFACE SLOSHING MODES

At the surface of a fluid, relatively large vertical motions are possible as shown in Figure 8. Pure sloshing motion does not involve volume change within the

fluid. The physical behavior of these modes involves the increase and decrease in the potential energy of the fluid at the surface. In addition, kinetic energy due to both the vertical and horizontal velocity of the fluid exists.

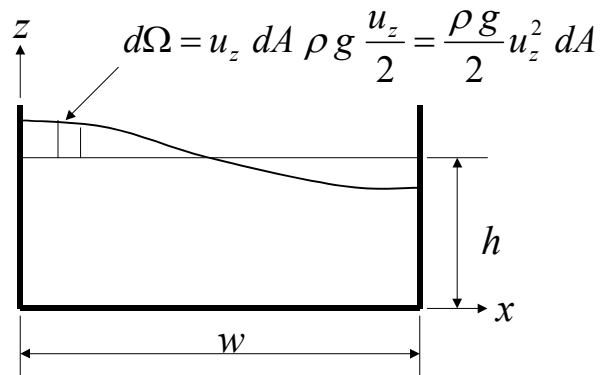


Figure 23.8. Surface Sloshing Behavior

The exact first mode frequency for the rectangular tank is given by [23.1]

$$\omega^2 = \frac{\pi g}{w} \tanh(\pi h / w) \quad (23.17)$$

For $w = h$ the first sloshing frequency is $\omega^2 = 3.13 \frac{g}{h}$.

In general, the fluid pressure changes associated with the sloshing mode are very small and are often neglected in fluid-structure interaction problems solved by the finite element method. Within finite element models, however, the sloshing behavior can be easily included by the addition of vertical spring elements to the surface nodes on the fluid surface. From the potential energy equation shown in Figure 23.8 the stiffness value of the nodal spring must be ρg times the tributary surface area. The use of these surface springs will tend to reduce the number of long period modes within the finite element model. In order that these surface springs not to be activated during the application of gravity, a temperature increase can be applied in order to produce zero vertical displacement at the surface.

23.12 VERTICAL WAVE PROPAGATION

Due to the existence of the free surface of the reservoir water can move vertically due to horizontal boundary displacements. These vertical waves are coupled with the horizontal displacements, since the water pressure is equal in all directions. If no horizontal motion exists, resonant vertical waves can still exist with a displacement given by the following equation:

$$u_z(z,t) = U_n \sin\left(\frac{2n-1}{2h}\pi z\right) \sin(\omega_n t) \quad \text{for } n = 1, 2, 3 \dots \quad (23.18)$$

Note that the vertical shape function satisfies the boundary conditions of zero displacement at the bottom and zero pressure at the surface of the reservoir. Substitution of Equation 18 into the vertical wave equation, $\rho \ddot{u}_z = \lambda u_{z,zz}$, produces the following vertical frequencies of vibration:

$$\omega_n = \frac{2n-1}{2h}\pi V \quad \text{Or,} \quad f_n = \frac{2n-1}{4} \frac{V}{h} \quad (23.19)$$

Therefore, for a reservoir depth of 100 feet the first frequency is 11.8 cps and the second frequency is 34.4 cps. For a reservoir depth of 200 feet the first two frequencies are 5.9 and 17.2 cps. Also, these vertical waves do not have radiation damping (if the bottom of the reservoir is rigid) as in the case of the horizontal waves propagating from the upstream face of the dam. The excitation of these vertical modes by horizontal earthquake motions is very significant for many dam-reservoir systems. However, silt at the bottom of the reservoir can cause energy absorption and reduce the pressures produced by these vertical vibration modes.

23.13 THE WESTERGAARD PAPER

Approximately seventy years ago Westergaard published the classical paper on “Water Pressure on Dams during Earthquakes” [23.2]. His paper clearly explained the physical behavior of the dam-reservoir interaction problem. The purpose of his work was to evaluate the pressure on Hoover dam due to earthquake displacements at the base of the dam.

Westergaard’s work was based on the solution of the simple two-dimensional reservoir/dam system, shown in Figure 9, subjected to horizontal earthquake displacement motion of $u_x(t) = u_{x0} \sin(\omega t)$ at the base of the dam.

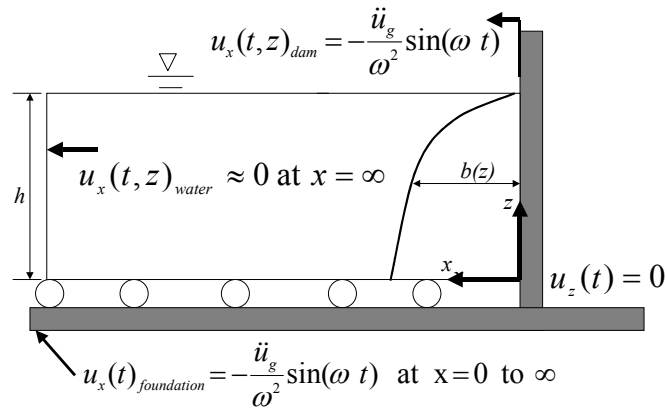


Figure 23.9. Rigid Dam and Reservoir Model

Since simple harmonic motion is assumed, the displacement is related to the acceleration by the following equation:

$$\ddot{u}_x(t) = -\omega^2 u_{x0} \sin(\omega t) \quad \text{Or, } u_{x0} = -\frac{\ddot{u}_x(t)}{\omega^2} \quad (23.20)$$

Westergaard solved the two dimensional compressible wave equations (Equations 7) by separation of variables. For a rectangular reservoir the solution is an infinite series of space and time functions. He then concluded (based on a 1.35 second measured period during the great earthquake in Japan in 1923) that *the period of earthquake motions (displacements) could be assumed to be*

greater than a second. Therefore, he assumed an earthquake period of 1.333 seconds, the exact compressibility of water and approximated the exact pressure distribution with a parabolic distribution. Based on these assumptions, Westergaard presented a conservative approximate equation for the pressure distribution for a rigid dam as

$$p(z) = \frac{7}{8} \sqrt{h(h-z)} \rho \ddot{u}_g = b(z) \rho \ddot{u}_g \quad (23.21)$$

where ρ is the mass density of water; or $\rho = w/g$. The term $b(z)$ can be physically interpreted as the equivalent amount of water that will produce the same pressure for a unit value of horizontal acceleration \ddot{u}_g of a rigid dam. The term *added mass* was never used or defined by Westergaard.

Theodor von Karman, in a very complimentary discussion of the paper, used the term apparent mass. Based on an incompressible water model and an elliptical pressure approximation he proposed the following equation for the pressure at the reservoir-dam vertical interface as

$$p(z) = 0.707 \sqrt{h(h-z)} \rho \ddot{u}_g = b(z) \rho \ddot{u}_g \quad (23.22)$$

One notes that the difference between the two approximate equations is not of great significance. Therefore, the assumption of 1.333 seconds earthquake period by Westergaard produces almost the same results as the von Karman solution.

Unfortunately, the term $b(z)\rho$ has been termed the added mass by others and has been misused in many applications with flexible structures using the relative displacement formulation for earthquake loading. All of Westergaard's work was based on the application of the absolute displacement of the earthquake at the base of the dam. For non-vertical upstream dam surfaces, some engineers have used this non-vertical surface pressure, caused by the horizontal earthquake motions, as an added mass in the vertical direction. The use of this vertical mass in an analysis due to vertical earthquake loading has no theoretical basis.

According to Westergaard, due to the high pressures at the base of the reservoir the water tends to *escape to the surface* of the reservoir. In addition, we will find in many reservoirs that the vertical natural frequencies are near the horizontal frequencies of the dam and the frequencies contained in the earthquake acceleration records.

23.14 DYNAMIC ANALYSIS OF RECTANGULAR RESERVOIR

A 100 foot depth, infinite-length reservoir is approximated by 100 by 300 feet finite element mesh shown in Figure 10. The deformed mesh for 2cps steady state harmonic displacement associated with one g acceleration is applied to the right boundary as shown in Figure 10. The water elements have a bulk modulus of 300,000 psi and a shear modulus of 30 psi. The upstream boundary of the reservoir is fixed horizontally or is modeled by pressure transmitting dashpots with a viscous constant of $c = \rho V = 5.296 \text{ #sec/in}^3$ per unit of boundary area. The “radiation boundary” solution was produced by a transient nonlinear analysis using the Fast Nonlinear Analysis method presented in Chapter 18.

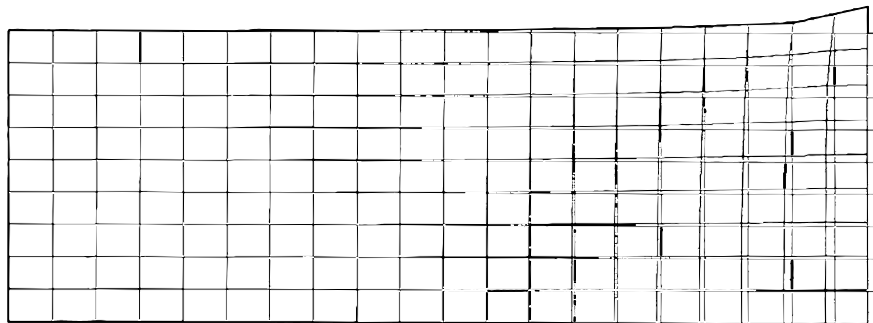


Figure 23.10. Deformed Mesh For 2 cps 1g Boundary Loading

Note that, for the 2cps low-frequency loading, the vertical displacement at the top of the reservoir is 4.89 inches significantly greater than the applied horizontal displacement 2.25 at the same point. This is due to the fact that the water near the right boundary has time to *escape* to the surface.

Assuming five percent modal damping and radiation boundary conditions, fluid pressures associated with the 2cps loading are shown in Figure 23.11.

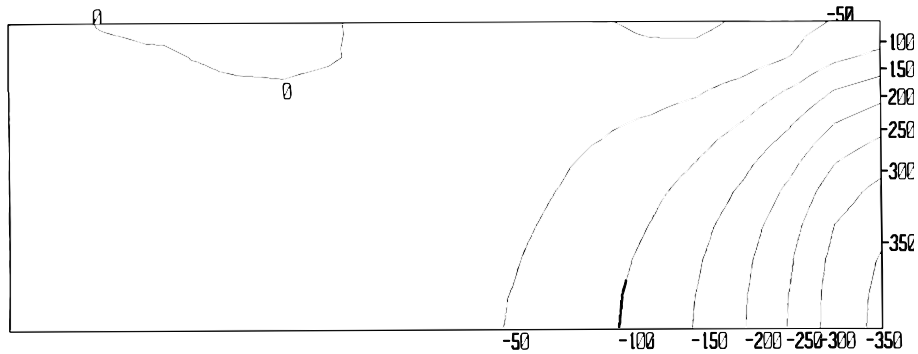


Figure 23.11. Pressure Distribution Times 10 for 2 cps 1g Boundary Loading

The maximum finite element pressure of 36.3 psi compares very closely with the added mass solution of 37.9 psi from Eq. (23.21). Because the finite element model has mass lumped at the surface, the zero pressure condition is not identically satisfied. A finer mesh near the surface would reduce this error.

The pressure distribution associated with 30 cps one g loading at the right boundary is shown in Figure 12. and illustrates the wave propagation associated with the 30 cps frequency loading. The apparent quarter wave length is approximately 120 feet. The exact one-dimensional, quarter-wave length associated with 30 cps in water is 33.25 feet. The difference is due to free-surface of the reservoir which allows vertical movement of the water. Of course the wave length associated with the incompressible solution is infinity.

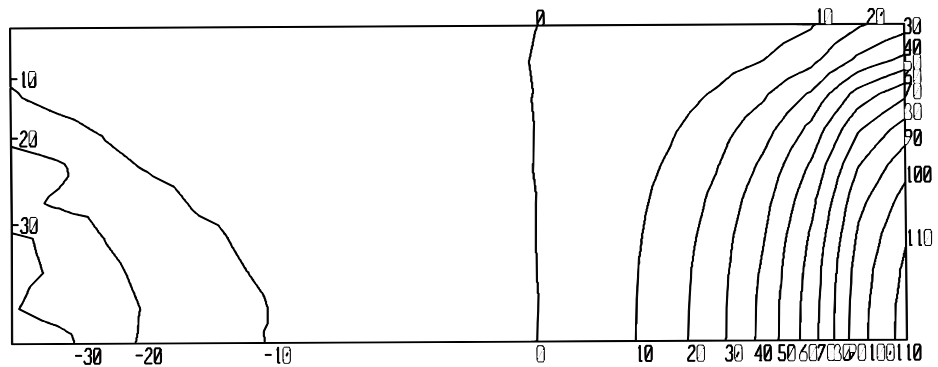


Figure 23.12. Pressure Distribution Times 10 for 30 cps 1g Boundary Loading

Table 23.4 summarizes the maximum pressure obtained using different boundary conditions at the upstream face of the reservoir and different values for modal damping. Since the loading is simple harmonic motion many different frequencies of the reservoir tend to be excited by all loadings. The first vertical frequency is 11.9 cps and the second vertical frequencies 34.4 cps. These partially damped resonant frequencies should not be excited to the same degree by typical earthquake type of loading which contain a large number of different frequencies.

**Table 23.4. Water Pressure vs. Frequency of Loading for a 300 ft. by 100 ft Reservoir
Added Mass Pressure Equals 37.9 psi for all Frequencies**

Loading Frequency CPS	Modal Damping Percent	Finite Element Fluid Model Maximum Pressures psi		Westergaard Compressible Solution No Damping psi	Confined One D. Wave Propagation No Damping psi
		Fixed Upstream Boundary	Radiation Upstream Boundary		
2	0.1	56.6	29.6	35.9	163.2
2	1.0	28.6	28.3	35.9	163.2
2	5.0	40.4	36.3	35.9	163.2
5	5.0	34.8	33.5	39.1	65.2
10	5.0	60.7	53.4	66.9	32.6
20	5.0	56.6	58.3	na	16.3
30	5.0	14.9	11.5	na	10.9

From this simp

Due to a singularity in the Westergaard solution the results are not valid for loading frequencies above 10 cps. However, from this simple study it is apparent that for low frequency loading, under 5 cps, the added mass solution is an acceptable approximation. However, for high frequencies, above 5 cps, the incompressible solution is not acceptable. For 30 cps the finite element pressure of 11.5 psi, is shown in Figure 12. At the bottom of the reservoir the finite element solution approaches the exact, wave-propagation solution of 10.9 psi for a confined one-dimensional problem. Normally, one would not expect that an

increase in damping, for the same loading, would cause an increase in pressure. However, this is possible as illustrated in Chapter 22.

23.15 ENERGY ABSORPTIVE RESERVOIR BOUNDARIES

In addition to the ability of the fluid finite element to realistically capture the dynamic behavior of rectangular reservoirs, it has the ability to model reservoirs of arbitrary geometry and the silt layer at the bottom of the reservoir. Table 23.6 summarizes measured reflection coefficients for bottom sediments and rock at seven concrete dams [23.4].

Table 23.6. Measured Reflection Coefficients for Several Dams

Dam Name	Bottom Material	α
Folsom	Bottom Sediments With Trapped Gas, Such As From Decomposed Organic Matter	-0.55
Pine Flat	Bottom Sediments With Trapped Gas, Such As From Decomposed Organic Matter	-0.45
Hoover	Bottom Sediments With Trapped Gas, Such As From Decomposed Organic Matter	-0.05
Glen Canyon	Sediments	0.15
Monticello	Sediments	0.44
Glen Canyon	Rock – Jurassic Navajo Sandstone	0.49
Crystal	Rock – Precambrian Metamorphic Rock	0.53
Morrow Point	Rock – Biotite, Schist Mica Schist, Micaceous Quartzite, And Quartzite	0.55
Monticello	Sandstone Interbedded With Sandy Shale And Pebbly Conglomerate	0.66
Hoover	Rock Canyon Walls	0.77

It is apparent that the reflection coefficient is a function of the thickness and properties of the bottom sediment and the properties of the underlying rock at a specific location within the reservoir.

The reflection coefficient α is the ratio of the “reflected” to “incident” wave amplitudes. The value of α varies between 1 and -1 . If $\alpha = 1$, the boundary is rigid and does not absorb energy and the wave is reflected 100 percent back into

23-26 STATIC AND DYNAMIC ANALYSIS

the reservoir. If $\alpha = 0$, the energy is completely dissipated and there is no reflection. If $\alpha = -1$, the boundary is very soft, compared to the bulk modulus of water, and does not absorb energy and the wave is reflected 100 percent back into the reservoir with a phase reversal.

Figure 23.13 illustrated two possible finite element models to simulate the dynamic behavior at the interface between the reservoir and boundary.

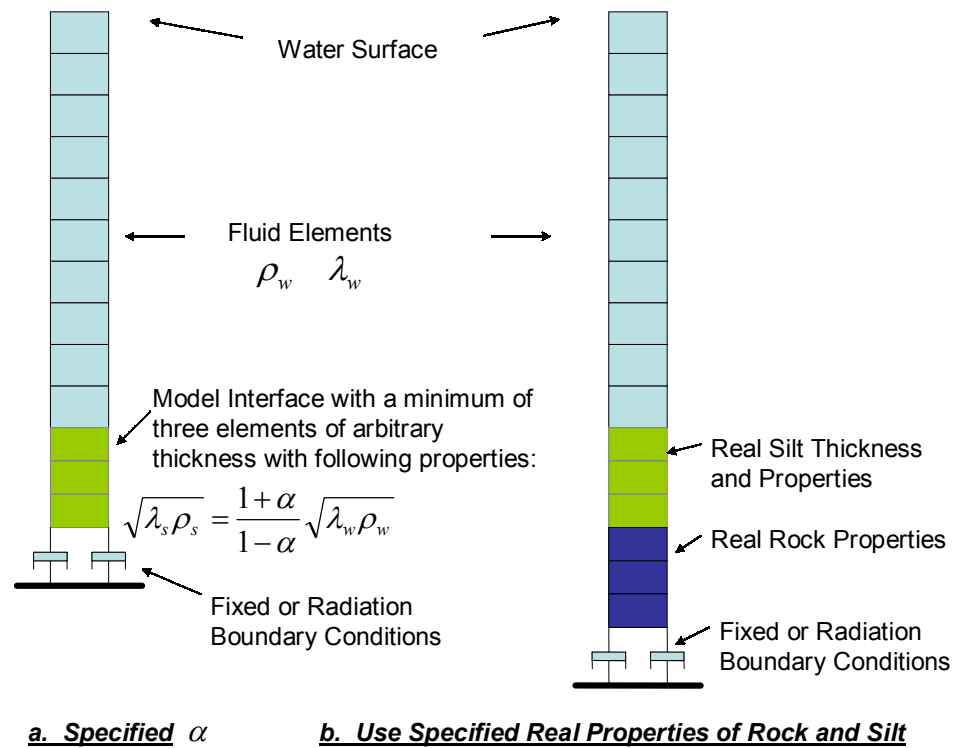


Figure 23.13. Two Possible Reservoir Boundary Models

Many special purpose computer programs for dam analysis allow a specification of reflection coefficients at the interface between the underlying rock and the reservoir. However, for most dam structures the deformation within the rock foundation must be included within the basic finite element model of the dam. Therefore, the preferable approach is to accurately model the sediment with finite elements. This approach allows the transfer of energy to the underlying rock to take place according to the basic laws of mechanics.

Shown in Figure 23.13a is a model where the silt and foundation properties are calculated from a specified α . The material properties of the silt layer must be calculated from Equation 23.15. Note that values of the bulk modulus and density are not unique. A realistic assumption is to select the density equal to or greater than the density of water.

A more general finite element model for the base and walls of the reservoir is shown in Figure 13b. If a significant amount of the rock foundation is modeled, using large elements, it may not be necessary to use radiation boundary conditions as illustrated in Chapter 16.

23.16 RELATIVE VERSUS ABSOLUTE FORMULATION

A two-dimensional view of a typical dam-foundation-reservoir-gate system, subjected to absolute earthquake displacements, was shown in Figure 1. However, if foundation-dam interaction is to be considered it is necessary to formulate the analysis in terms of the displacements relative to the free field displacements that would be generated without the existence of the dam and reservoir. Figure 23.6 illustrates the type of loading that is required if a relative displacement formulation is used.

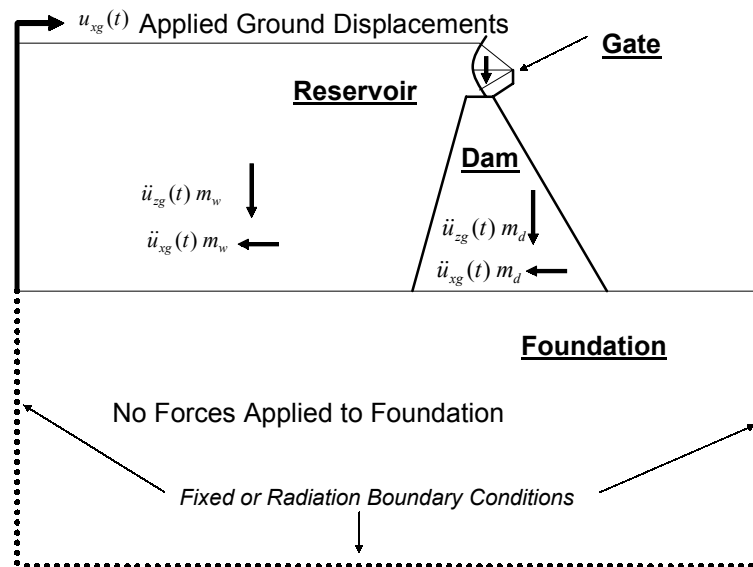


Figure 23.14. Relative Displacement Formulation of Dam-Reservoir System

It can easily be shown, for the relative displacement formulation, that the loading on the reservoir, dam and gate is the mass times the ground acceleration. In

23-30 STATIC AND DYNAMIC ANALYSIS

order to simulate the upstream reservoir boundary condition it is necessary to apply the negative horizontal ground displacements to the upstream face of the reservoir in addition to inertial loading on the water elements. If the foundation of the system is included, no inertial load is applied to the foundation elements. However, the mass of the foundation must be included in the evaluation of the shape functions to be used in the mode superposition dynamic analysis of the complete system

23.17 THE EFFECT OF GATE SETBACK ON PRESSURE

Radial gates are normally set back from the upstream face of the dam as shown in Figure 23.15. One question that requires an answer is: *does the setback increase or decrease the pressure acting on the gate?* Also, *how does one create a finite element model of the reservoir in order to avoid the displacement singularity at the intersection of the upstream face of the dam and the approximately horizontal spillway?*

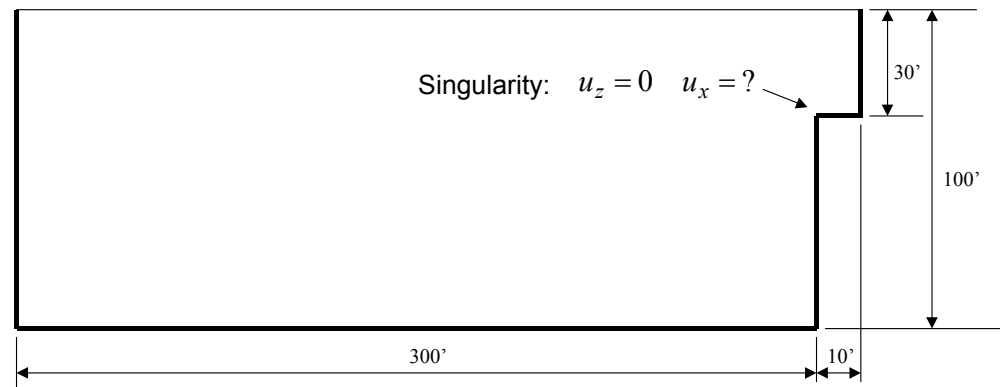


Figure 23.15. Reservoir With Radial Gate Setback

The second question must be addressed first in order to evaluate the effects of the setback on the pressure distribution. Due to the applied displacements at the right boundary, there should be a relatively large vertical displacement at this intersection; however, due to the existence of the horizontal surface the vertical water displacement should be zero. In addition, the horizontal displacement of the water must be equal to the applied displacement; however, the horizontal movement of the water on top of the spillway must be allowed to move horizontally if the correct pressures are to be developed at the base of the gate. One can approximate this behavior by reducing the stiffness of the water element near this singularity. A preferable approach is to create additional nodes at the singular point and to allow the discontinuity in displacements to exist. A finite element mesh, that satisfies these requirements, is shown in Figure 23.16.

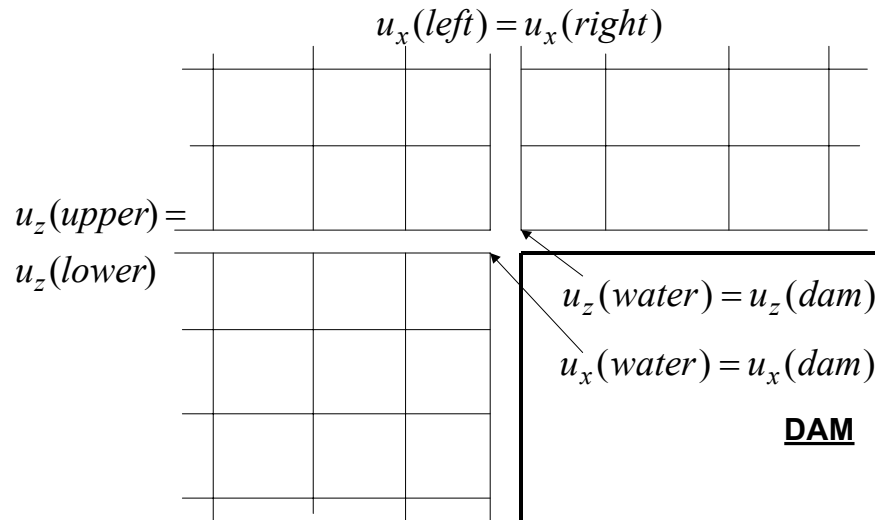


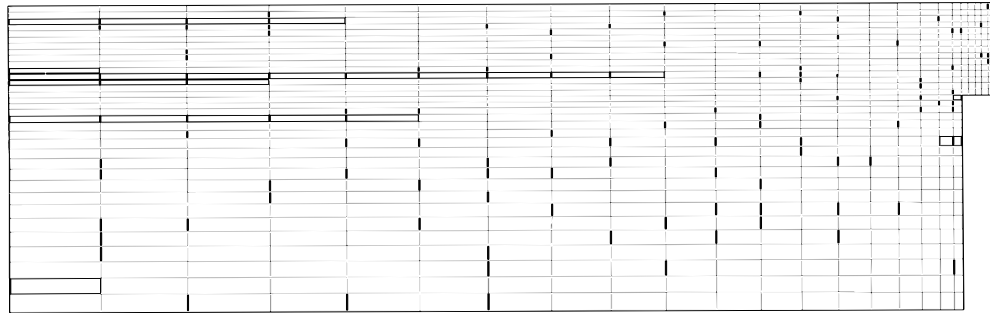
Figure 23.16. Suggested Mesh at Intersection of Upstream and Spillway Surfaces

Inserting shear-free horizontal and vertical interfaces between the dam and reservoir and between different areas of the reservoir allows all boundary conditions to be satisfied. Note that it is not necessary to add additional elements. However, the vertical displacements will not be equal on the two sides of the vertical interface and the horizontal displacement will not be equal at the top and bottom of the horizontal interface. Near the surface several of the fluid nodes on the vertical fluid may be constrained to have the same vertical and horizontal displacements in order that the surface displacements are continuous.

The finite element mesh used to study the setback problem is shown in Figure 23.17. The maximum pressures due to a 2 cps 1 g boundary loading with zero damping and no radiation damping, are summarized in Table 23.6 for the cases of with and without gate setback.

Table 23.6. Summary of Pressures With and Without Gate Setback

	With Gate Setback	Without Gate Setback
Pressure at Base of Gate	16.5 psi	20.6 psi
Pressure at Base of Dam	31.9 psi	33.6 psi



From this simple example it is apparent that the setback of the gate from the upstream face of the dam reduces the pressures acting on the gate and at the base of the dam. Since the setback increases the surface area of the reservoir, the water below the base of the gate can escape to the surface more easily; therefore, all pressures are reduced.

Figure 23.17. Finite Element Mesh for Reservoir with Gate Setback

23.18 SEISMIC ANALYSIS OF RADIAL GATES

A significant number of seismic analyses of radial gates have been conducted based on a two stage dynamic analysis. First the dam, without the gate, is analyzed for the specified ground motions. In most cases the added mass approach is used to approximate the dynamic behavior of the dam and reservoir. The acceleration obtained from this analysis, at the location of the gate, is then applied to a separate finite element model of the gate only. The reservoir associated with gate is approximated by an added mass calculated using the total depth of the reservoir. The model of the gate, with the reservoir added mass, is then subjected to the accelerations history (or the corresponding response spectra) calculated from the dam analysis model.

In many cases the two dynamic analyses are conducted using different computer programs. This is because many special purpose dam analysis programs do not contain three dimensional frame and shell elements that are required to accurately model the steel gates. In addition, the two stage dynamic analysis is based on incompressible fluid and rigid structure assumptions.

During the past three years the author has conducted several seismic analyses of several dam-reservoir-gate systems using one model where the reservoir has been modeled by compressible fluid elements and the gate accurately modeled by beam and shell elements [3]. In addition to the improved accuracy of this approach there is significant reduction in the amount of manpower in the preparation of only one model. Also, there is no need to calculate added mass and it is not necessary to transfer the output from one dynamic analysis as the input data for a separate gate model. Therefore, the one three-dimensional dynamic analysis is simpler than the commonly used two stage approach. The computer time requirements for the dynamic analysis of this comprehensive model are approximately one hour using an inexpensive personal computer. However, the preparation and verification of a large finite element model still requires a significant amount of engineering time. Therefore, there is a motivation to use a more simplified model to evaluate the seismic safety of radial gates. The following is a list on modeling assumptions that may help to reduce the amount of manpower required to prepare the finite element model:

1. We have found that a fine mesh, shell-element model of the gate and support beams is necessary in order to capture the complex interaction of the face of the gate with the backup beam structure. This level of detail is necessary to match the measured frequencies of the dry gate, and to produce realistic stresses in the gate structure. The arms and diagonal braces of the gate can be modeled with frame elements that neglect secondary bending stresses within the one-dimensional elements.
2. We found that both the dry and wet frequencies of a typical gate are high and do not significantly affect the total dynamic loads on the gate and trunnion. For the gate studied in reference [3], it was found that if the modulus of elasticity of the steel of the gate was doubled, the maximum earthquake reaction at the trunnion was increased by less than 10 percent. Therefore, it may be possible to use a coarse finite element mesh to model the face of the gate, along with a three-dimensional model of the reservoir and dam, to obtain the maximum dynamic pressure acting on the gate.
3. A second option for simplifying the modeling is based on the fact that the dynamic pressure distribution was found to be approximately the same at the center and at the edges of the gate, indicates that a coarse mesh, along the axis of the gate, can be used to model the reservoir upstream of the gate. It appears that excellent results can be produced if fewer layers of reservoir elements are used along the horizontal axis of the gate.
4. Formal constraint equations can be used to connect the fine mesh gate to the coarse mesh reservoir. However, the steel gate is very stiff compared to the stiffness of water; therefore, the fine mesh steel elements will automatically be compatible with the coarse mesh water elements and formal constraint equations are not required.
5. This approach of using a coarse mesh reservoir and fine mesh gate model in the same analysis appears to be more accurate and will require less engineering time than the approximate two stage analysis suggested in the previous paragraph. Physically, this approximation is similar to lumping the water mass at the coarse mesh nodes between the gate and reservoir. Therefore, these nodes should be located at nodes on the face of the gate

where the ribs and beams exist. This approximation neglects bending stresses in the face plate between the ribs. However, one can approximately calculate these additional bending stresses from simple beam equations. Or, one can ignore these bending stresses since local yielding in the face plates will not cause the failure of the gate.

6. For a straight gravity dam the same number of layers used to model the reservoir should be used to model the dam and foundation. This plane model, coupled with a fine-mesh, three-dimensional, shell/beam model of the gate, should produce acceptable results. It is important that the maximum depth of the reservoir below the gate is used for the plane model. A three-dimensional model of the dam and reservoir, including the V-shape of the canyon, will produce lower pressures on the gate. Therefore, this “planar slice” should be conservative. Vertical earthquake motions applied to this model should produce conservative water pressures, since the water is constrained from lateral movement in this formulation
7. For an arch or curved dam a three-dimensional, coarse mesh model of the dam, foundation and reservoir should be created in order to accurately capture the complex dynamic interaction between the reservoir, dam and foundation. The coarse mesh model can be coupled with a fine mesh model of a typical gate. The combined system can be subjected to all three components of earthquake displacements and the resulting analysis should be realistic since a minimum number of approximations have been introduced.
8. After a careful study of the dynamic behavior of the water above the spillway, between the upstream face of the gate and the upstream face of the dam, it appears that this volume of water can be eliminated from the reservoir model. This can be accomplished by moving the fine mesh model of the gate and trunnion upstream so that the base of the face of the gate is at the same location as the upstream face of the dam. This assumption will simplify the model and allow the water to move freely in the vertical direction during dynamic loading and transfer reservoir pressure fluctuations directly to the gate structure. Parameter studies have indicated that this approximation produces slightly conservative results. Stiff link elements,

normal to the upstream face of the dam and radial gate, must be used to connect the reservoir and structure.

9. A horizontal boundary, with two nodes at the same location, should be located at the elevation of the contact between the gate and spillway and extend to the upstream boundary of the reservoir. These nodes should have equal vertical displacements and independent horizontal displacements. This will allow the bottom of the gate to move relative to the top of the spillway. The same type of boundary should exist between the foundation and the reservoir.

23.19 FINAL REMARKS

The classical approximation of incompressibility was first introduced to simplify the mathematics in order to obtain a closed form mathematical solutions of fluid dynamics problems with simple geometry. In addition, added mass approximation is valid only for low frequencies under 5 cps. However, these approximations are not required at the present time due to the development of three-dimensional fluid elements, inexpensive, high-speed computers and other efficient numerical method of dynamic analysis. Also, dam/reservoir/gate/foundation systems of arbitrary geometry can all be included in the same model.

Viscous forces within the fluid and the frictional forces between the dam-foundation-gate and the reservoir have been neglected. Therefore, the assumption of five percent damping appears to be a reasonable approximation until further research is conducted. It may be worthwhile to conduct an analysis of a two dimensional, computational fluid dynamic analysis of a reservoir only, where the real viscosity of the water is included in order to verify that equivalent modal damping can be used to approximate the viscous energy dissipation. Additional experimental research and parameter studies for one and two dimensional finite element models must be conducted to evaluate the sensitivity of all damping assumptions.

The upstream reservoir mesh should be approximately four times the maximum depth of the reservoir. If foundation deformations are significant, the foundation

mesh should extend downstream and below the dam a distance equal to two times the upstream/downstream width of the base of the dam. Inertia loads should not be applied to the foundation elements. However, the foundation mass must be included in the calculation of the mode shapes.

The mesh should be coarse at the base and near the upstream vertical boundary of the reservoir. The finest mesh, in both the horizontal and vertical directions, should be near the upstream face or the dam or gate.

The finite element fluid model and boundary conditions must be verified by the application of vertical dead load to the reservoir. The total horizontal hydrostatic force applied to the face of the dam and gate can be calculated from static equilibrium equations and should be within few percent of the finite element solution. In addition, the stresses (pressure) within the water elements σ_x , σ_y and σ_z should be approximately equal. Also, the hydrostatic pressure at the base of the reservoir, obtained from the finite elements model, should be very close to the weight of a unit area of water above the node.

After the static model is verified by the plotting of stresses and deflected shapes, the natural eigenvectors, including both static and dynamic modes, should be calculated and plotted. Both the total static and mass participation factors should be examined. One hundred percent static participation is required and over ninety percent of the mass participation in all the directions of earthquake loading is required to assure a converged solution.

23.20 REFERENCES

1. Cook, R., D. Malkus and M. Plesha, "Concepts and Applications of Finite Element Analysis", Third Edition, John Wiley and Sons, Inc., 1989.
2. Westergaard, H. M. "Water Pressure on Dams During Earthquakes", Transactions, ASCE, Vol. 9833, Proceedings November 1931.
3. Aslam M., Wilson E.L., Button M. and Ahlgren E., "Earthquake Analysis of Radial Gates/Dam Including Fluid-Structure Interaction," Proceedings, Third

U.S.-Japan Workshop on Advanced Research on Earthquake Engineering for Dams, San Diego, CA. June 2002.

4. Engineering Guidelines for the Evaluation of Hydropower Projects, Federal Energy Regulatory Commission.